

## MORPHOLOGICAL AND OPTICAL PROPERTIES OF FUNCTIONALIZED SWCNTs:P3OT NANOCOMPOSITE THIN FILMS, PREPARED BY SPIN-COATING

J. AL-ZANGANAWEE<sup>a,b</sup>, M. AL-TIMIMI<sup>b,c</sup>, A. PANTAZI<sup>a,c</sup>,  
O. BRÎNCOVEANU<sup>a,c</sup>, C. MOISE<sup>a</sup>, R. MESTERCA<sup>a</sup>, D. BALAN<sup>a,c</sup>,  
S. IFTIMIE<sup>c</sup>, M. ENACHESCU<sup>a,d\*</sup>

<sup>a</sup>*Center for Surface Science and Nanotechnology (CSSNT), University Politehnica of Bucharest, Romania*

<sup>b</sup>*Physics Department, College of Science, University of Diyala, Iraq*

<sup>c</sup>*University of Bucharest, Faculty of Physics, Bucharest, Romania*

<sup>d</sup>*Academy of Romanian Scientists, Bucharest, Romania*

We report the fabrication of nanocomposite thin films based on regio-regular polymer poly(3-octylthiophene-2,5-diyl) (P3OT) and functionalized single wall carbon nanotubes (F-SWCNTs) using three different filler mass concentration (3, 6 and 12 wt., %), by spin-coating technique. Morphological and optical investigations were performed and the obtained results were compared with those of P3OT individual layer. The thermogravimetric measurements confirmed the successful functionalization of the SWCNTs. However, field emission scanning electron microscopy (FE-SEM) and high resolution scanning electron microscopy (HR-SEM) images showed the presence of bundles, with different diameters. Nevertheless, percentages of amorphous carbon and metallic catalysts have smaller values for functionalized SWCNTs compared with the pristine samples. An increase in optical absorption with the increase of F-SWCNTs added amount was observed, while the bandgap energy values of our fabricated nanocomposite structures slightly decreased. Our studies proved that the optimal added amount of F-SWCNTs should not exceed 6 wt., %, otherwise the nanotubes will be pushed onto the surface of the customized structure.

(Received June 6, 2016; Accepted July 22, 2016)

*Keywords:* SWCNTs, P3OT, TGA, FE-SEM, HR-STEM, micro-Raman, nanocomposite

### 1. Introduction

Since Iijima & Ichihashi [1], and Bethune and his collaborators [2], working independently, reported the discovery of single wall carbon nanotubes (SWCNTs) based on innovative studies done by Iijima in 1991 [3], when for the first time the structure of multi-wall carbon nanotubes (MWCNTs) was presented, the gates of nanoscience and nanotechnology were opened [4]. Particularly, SWCNTs offer a unique structure with diameters in 1.0 – 1.5 nm range and length of tens of microns [4], providing remarkable electric, mechanical, optical and chemical properties. Due to this particular structure, SWCNTs are highly sensitive to chemical changes and doping [4] allowing their use in many and various applications like transistors [5-7], biology and medicine [8-10] or photovoltaic structures [11-14]. In recent years, conductive polymers – SWCNTs mixture based photovoltaic cells received special attention from scientific community due to high photoconductivity values of SWCNTs [15, 16] and easy fabrication techniques [17, 18]. Thereby, the presence of SWCNTs in the architecture of various organic photovoltaic cells as interlayer [19, 20] or as active film improved the charge carriers' separation and their transport to electrodes [21].

---

\* Corresponding author: marius.enachescu@upb.ro

Moreover, PV industry has grown exponentially in the last 20 years and important amounts of time and money were invested in so called “green energy”, especially after the discovery of conjugated polymers which can be considered a milestone of organic photovoltaic field [22]. Special attention was paid to poly(3-octylthiophene-2,5-diyl) (P3OT) and poly(3-hexylthiophene-2,5-diyl) (P3HT),  $\pi$ -conjugated polymers that proved to have an early crystalline structure as thin films, facilitating the charge carriers’ transport [23, 24]. Huge number of papers were dedicated to conjugated polymer:fullerene derivative as active layer of organic photovoltaic cells, opposite to conjugated polymer:SWCNTs hybrid structures.

In this paper we report results of morphological and optical studies dedicated to functionalized SWCNTs:P3OT thin films, taking into account three weight ratios of F-SWCNTs (3, 6 and 12 wt., %).

## 2. Experimental procedures

### 2.1 Materials

SWCNTs with diameters in 0.9 – 1.7 nm range and length from 300 nm to 4  $\mu$ m were purchased from NanoIntegris Inc and were functionalized using nitric acid solution (6M HNO<sub>3</sub>). The initial purity of single wall carbon nanotubes was indicated to be 70%. P3OT was purchased from Sigma Aldrich Company and used without further improvements.

The obtaining of P3OT:F-SWCNTs solution, varying the weight ratio of F-SWCNTs (3, 6 and 12 wt., %), was a two-step procedure. First step consisted in the dispersion of F-SWCNTs in chloroform, and in the second step P3OT and F-SWCNTs components were blended. To achieve an optimal homogeneity, the resulting solution was mixed for 1h at 50°C. Our nanocomposite thin films were deposited onto optical glass substrates, by spin-coating, at room temperature, in air. Before deposition procedure, the substrates were cleaned with acetone, isopropyl alcohol and deionized water using a sonication bath for 15 minutes. The optimal thickness of organic photovoltaic cells active layer should exceed the exciton diffusion length [25] and in order to obtain such films the working parameters in our fabrication process were as following: the angular speed was 1000rpm and deposition time was 30 seconds. For our deposited nanocomposite thin films the thickness was determined to be around 110 nm.

### 2.2 Characterization techniques

Micro-Raman spectroscopy analyses of the pristine and functionalized SWCNTs were performed at room temperature using a Horiba HR800 system with a He-Ne laser with 2.33 eV energy, 532 nm wavelength, 2  $\mu$ m diameter of laser spot, and 600 lines/mm grating. Raman measurements were performed in the 75 cm<sup>-1</sup> - 3000 cm<sup>-1</sup> range. Thermogravimetric analyses (TGA) were used to quantize the mass loss of materials induced by temperature. A STA-8000 Perkin Elmer instrument was used, operating in 50°C – 900°C temperature range and 5°C/minute heating rate. Morphological features of our fabricated P3OT:F-SWCNTs nanocomposite thin films were studied by field emission scanning electron microscopy (FE-SEM) and high resolution scanning transmission electron microscopy (HR-STEM). Optical investigations were performed in visible range, from 400 nm to 800 nm, at room temperature.

## 3. Results and discussion

### 3.1 Raman investigations

Raman spectra of pristine and F-SWCNTs are presented in figure 1. Radial breathing mode (RBM) region, localized in 150 cm<sup>-1</sup> – 300 cm<sup>-1</sup> range for both samples, is slightly shifted to shorter wavelengths for F-SWCNTs. Disorder induced mode peaks (D-band) are attributed to  $sp^3$  carbon atoms, while G-band corresponding to tangential modes is related with in-plane oscillations of  $sp^2$  hybridized carbon atoms [26, 27]. For functionalized single wall carbon nanotubes, disorder increased most likely due to nitric acid treatment inducing localized defects on the sidewall structure. This approach is confirmed by a strongly decrease of I<sub>G</sub>/I<sub>D</sub> ratio value of F-SWCNTs.

( $I_G$ ) and ( $I_D$ ) are the maximum intensities peaks of the G-band and D-band, respectively and  $I_G/I_D$  ratio gives information about structural changes induces by functionalization procedure, like attachment of various organic moieties [28-30].

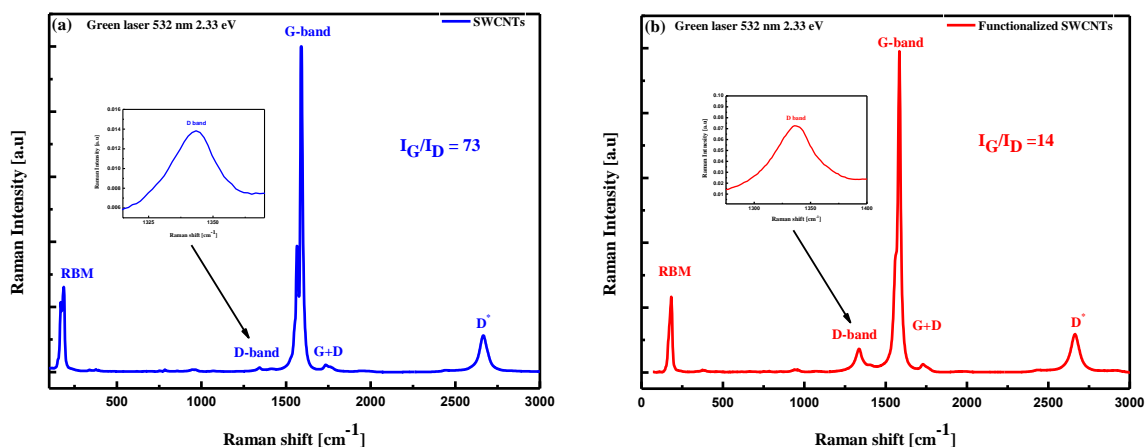


Fig.1. (a) Raman spectrum of pristine SWCNTs and (b) Raman spectrum of F-SWCNTs recorded using green light laser with 532 nm wavelength and 2.33 eV energy. D-Band of F-SWCNTs is bigger than D-Band of pristine SWCNTs, and the  $I_G / I_D$  ratio of F-SWCNTs is lower than the  $I_G / I_D$  ratio of pristine SWCNTs.

### 3.2 Thermogravimetric measurements

TGA analyses are usually used to determine the mass loss induced by temperature, to quantize the metal catalysts ratio or to study the purity of single wall carbon nanotubes [28]. Also, as in our case, these kinds of studies give information about the success rate of the functionalization process. Our TGA curves for both pristine and F-SWCNTs are presented in figure 2, together with their derivatives.

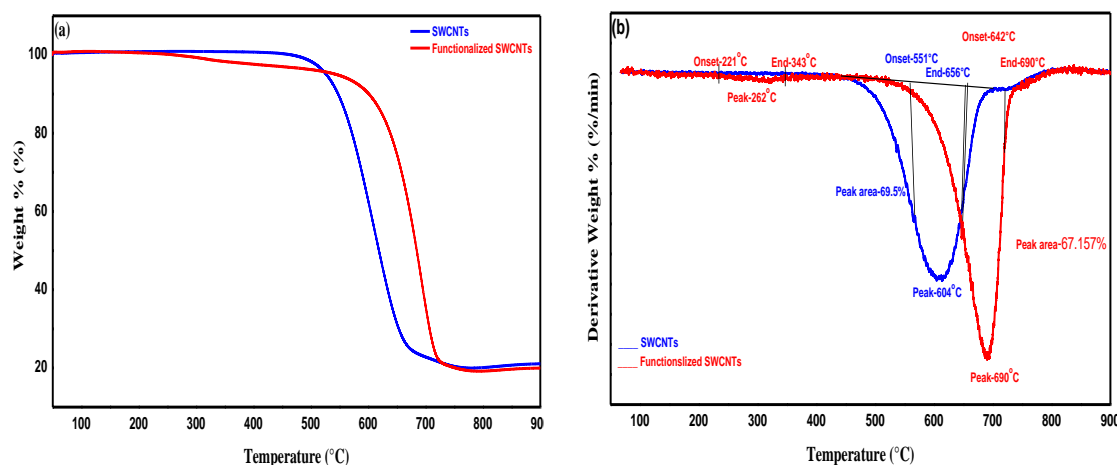


Fig. 2. (a) TGA curves and (b) its derivatives of pristine and functionalized SWCNTs, recorded in air.

For F-SWCNTs the onset burning temperature is lower than for the pristine ones, indicating, as other authors observed [31], the presence of various organic moieties attached to sidewalls or to the ends of the structure.

Also, TGA measurements were performed for P3OT:F-SWCNTs thin films, taking into account different weight ratios of F-SWCNTs (3, 6 and 12 wt., %), and the results were compared

with those obtained for F-SWCNTs and P3OT individual layers. These spectra are depicted in figure 3 and showed the successful incorporation of F-SWCNTs into polymer matrix. The increase in F-SWCNTs percentage of P3OT:F-SWCNTs nanocomposite layers leads to an increase of metal catalysts ratio.

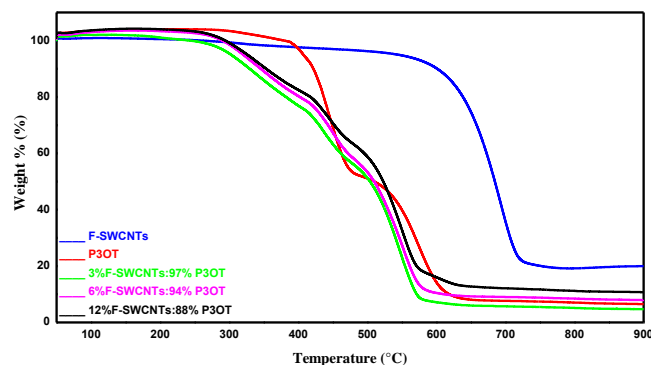


Fig. 3. TGA curves of P3OT, SWCNTs and P3OT:F-SWCNTs thin films, taking into account various percentages of functionalized single wall carbon nanotubes for our composite layers (3, 6 and 12 wt., %).

### 3.3 Morphological features

FE-SEM and HR-STEM images of our functionalized SWCNTs are presented in figure 4.

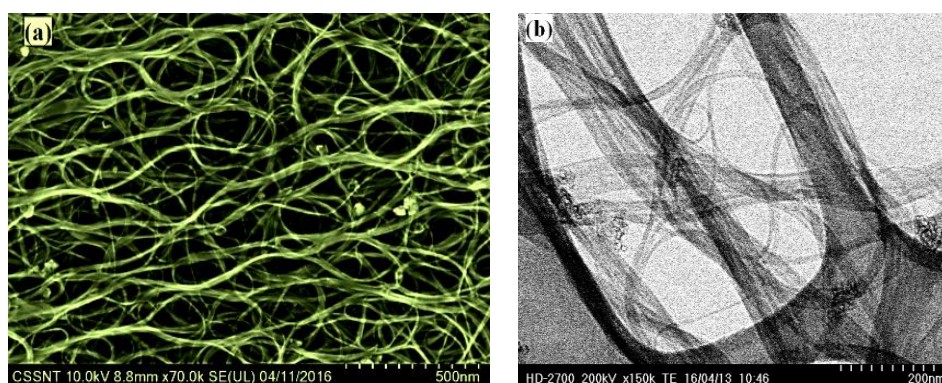
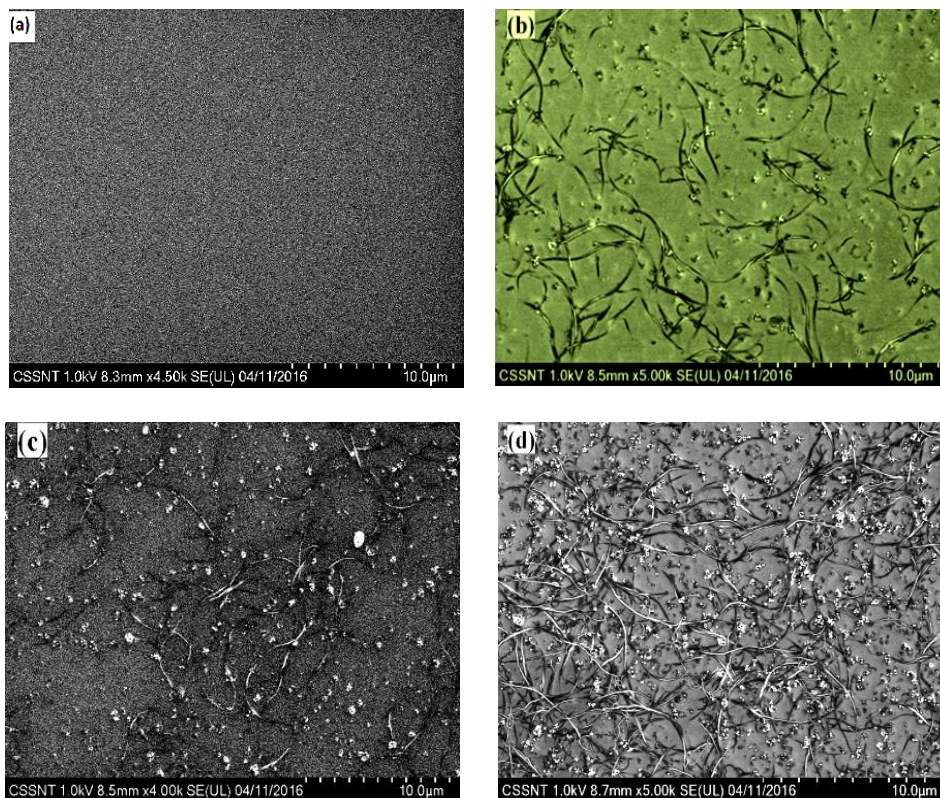


Fig. 4. (a) FE-SEM and (b) HR-STEM images of our fabricated functionalized single wall carbon nanotubes.

Despite a successful functionalization proved by TGA measurements, a high density of bundles, with different diameters, can be observed from FE-SEM image of functionalized single wall carbon nanotubes, which are a result of the well-known high van der Waals interactions present between the nanotubes [32].

The FE-SEM images of P3OT:F-SWCNTs nanocomposite thin films, for different percentages of functionalized single wall carbon nanotubes, 3, 6 and 12 wt., %, are presented in figure 5, and these results are compared with those obtained for P3OT individual layer. TGA curves confirmed the entrainment of F-SWCNTs into polymer matrix, but the FE-SEM images showed that the optimal percentage should not exceed 6%, otherwise most of the nanotubes will be pushed onto the surface of polymer film, as can be observed in figure 5(d). The FE-SEM image of P3OT individual thin film showed a very uniform and smooth surface, a specific feature of layers deposited by spin-coating technique, suitable for use in the architecture of photovoltaic cells as component of the active layer.



*Fig. 5. FE-SEM images of P3OT:F-SWCNTs nanocomposite thin films with different percentages of F-SWCNTs: (b) 3%, (c) 6% and (d) 12%. The obtained results were compared with those of (a) P3OT individual layer.*

### 3.4 Optical characterization

Optical absorption spectra of P3OT:F-SWCNTs nanocomposite thin films, with different F-SWCNTs percentages (3, 6 and 12 wt., %), together with the results obtained for P3OT individual layer, were drawn in visible range, at room temperature, and are depicted in figure 6.

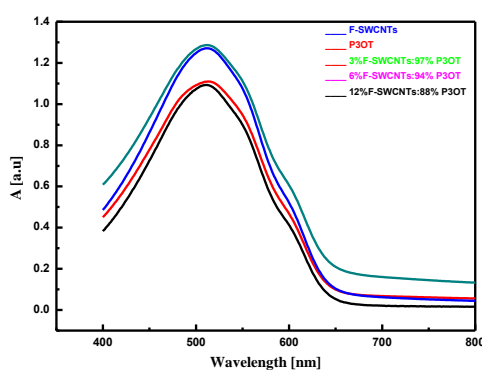


*Fig. 6. Optical absorption of P3OT:F-SWCNTs nanocomposite thin films with different percentages of F-SWCNTs (3, 6 and 12 wt., %). The obtained results were compared with those of P3OT individual layer.*

An increase in optical absorption with the increase of F-SWCNTs added amount was observed, which confirms the improvement of charge carriers' transfer between the SWCNTs and organic materials observed also by other authors [19, 20]. Moreover, a slight decrease of optical bandgap energy values was determined with the increase of F-SWCNTs added amount, as

following: 2.14 eV for P3OT individual layer, 2.11 eV for P3OT:F-SWCNTs (3 wt., %), 2.07 eV for P3OT:F-SWCNTs (6 wt., %) and 2.05 eV for P3OT:F-SWCNTs (12 wt., %). Most likely, this behavior can be associated with the increase of the number of localized states in the forbidden band of our customized structure [33]. These results proved that F-SWCNTs added into the polymer matrix can be used as constitutive in the architecture of various hybrid photovoltaic cells. Moreover, usually for nanoscale electronic and optoelectronic devices Schottky junctions are found between carbon nanotubes and different organic materials.

#### 4. Conclusions

Compositional, morphological and optical properties of the F-SWCNTs and P3OT nanocomposite thin films at different filler mass concentration (3, 6, 12 wt., %), obtained by spin-coating, were studied and compared with P3OT individual layer. Although the TGA analysis of the samples demonstrated the successful functionalization of the SWCNTs, the electron microscopy images of the nanocomposites showed the all-ready known preferential arrangement of the nanotubes into bundles of different diameters.

The optimal added mass of SWCNTs was demonstrated to be equal or less than 6 wt., % by the FE-SEM images otherwise the carbon nanotubes will be pushed onto the thin film surface. Optical investigations showed that absorbance of our fabricated thin films increases with the increase of F-SWCNTs added amount, while determined bandgap values decreased, most likely due to the increase number of localized states in the forbidden band of the customized structure. These results confirmed that F-SWCNTs can be integrated in the architecture of electronic and optoelectronic devices, especially for photovoltaic cells, but further studies are required to fully understand the physical processes involved.

#### Acknowledgements

This work was supported by Romanian Ministry of Education and Scientific Research and by Executive Agency for Higher Education, Research, Development and Innovation, under Projects PCCA 166/2012 and ENIAC 04/2014. J. Al-Zanganawee and M. AL-Timimi acknowledges the support of the Ministry of Higher Education and Scientific Research of Iraq and University of Diyala.

#### References

- [1] S. Iijima, T. Ichihashi, *Nature* **363**, 603 (1993)
- [2] D.S. Bethune, C.H. Kiang, M.S. Devries, *Nature* **363**, 605 (1993)
- [3] S. Iijima, *Nature* **354**, 56 (1991)
- [4] W. Zhou, X. Bai, E. Wang, S. Xie, *Advanced Materials* **21**, 4565 (2009)
- [5] Z.H. Chen, J. Appenzeller, J. Knoch, Y.M. Lin, P. Avouris, *Nano Letters* **5**, 1497 (2005)
- [6] M. Ganzhorn, A. Vijayaraghavan, S. Dehm, F. Hennrich, A.A. Green, M. Fichtner, A. Voigt, M. Rapp, H. von Lohneysen, M.C. Hersam, M.M. Kappes, R. Krupke, *ACS Nano* **5**, 1670 (2011)
- [7] B.L. Liu, C. Wang, J. Liu, Y.C. Che, C.W. Zhou, *Nanoscale* **5**, 9483 (2013)
- [8] S. Diao, G. Hong, J.T. Robinson, L. Jiao, A.L. Antaris, J.Z. Wu, C.L. Choi, H. Dai, *Journal of American Chemical Society* **134**, 16971 (2012)
- [9] H. Kosuge, S.P. Sherlock, T. Kitagawa, R. Dash, J.T. Robinson, H. Dai, M.V. McConnell, *Journal of American Heart Association* **1**, e002568 (2012)
- [10] A.L. Antaris, J.T. Robinson, O. Yaghi, G. Hong, S. Diao, R. Luong, H. Dai, *ACS Nano* **7**, 3644 (2013)
- [11] R.M. Jain, R. Howden, K. Tvrdy, S. Shimizu, A.J. Hilmer, T.P. McNicholas, K.K. Gleason, M.S. Strano, *Advanced Materials* **24**, 4436 (2012)

- [12] C.M. Isborn, C. Tang, A. Martini, E.R. Johnson, A. Otero-de-la-Roza, V.C. Tung, *The Journal of Physical Chemistry Letters* **4**, 2914 (2013)
- [13] L. Baschir, S. Antohe, A. Radu, R. Constantineanu, S. Iftimie, I.D. Simandan, M. Popescu, *Digest Journal of Nanomaterials and Biostructures* **4**, 1645 (2013)
- [14] T. Ishwara, D.D.C. Bradley, J. Nelson, P. Ravirajan, I. Vanseveren, T. Cleij, D. Vanderzande, L. Lutsen, S. Tierney, M. Heeney, I. McCulloch, *Applied Physics Letters* **89**, 252102 (2006)
- [15] J.U. Lee, P.J. Cordella, M. Pietrzkowski, *Applied Physics Letters* **90**, 053103 (2007)
- [16] N.M. Gabor, Z. Zhong, K. Bosnick, J. Park, P.L. McEuen, *Science* **325**, 1367 (2009)
- [17] L. Magherusan, P. Skraba, C. Besleaga, S. Iftimie, N. Dina, M. Bulgariu, C.G. Bostan, C. Tazlaoanu, A. Radu, L. Ion, M. Radu, A. Tanase, G. Bratina, S. Antohe, *J. Optoelectron. Adv. Mater.* **2**, 212 (2010)
- [18] T. Song, S.-T. Lee, B. Sun, *Journal of Materials Chemistry* **22**, 4216 (2012)
- [19] P.L. Ong, W.B. Euler, I.A. Levitsky, *Nanotechnology* **21**, 105203 (2010)
- [20] D. Ghosh, P. Ghosh, M.Z. Yusop, M. Tanemura, Y. Hayashi, T. Tsuchiya, T. Nakajima, *Physica Status Solidi RRL* **6**, 303 (2012)
- [21] S. Ren, M. Bernardi, R.R. Lunt, V. Bulovic, J.C. Grossman, S. Gradecak, *Nano Letters* **11**, 5316 (2011)
- [22] H. Shirakawa, E.J. Louis, A.G. MacDiarmid, C.K. Chiang, A.J. Heeger, *Journal of Chemical Society – Chemical Communications* **16**, 578 (1977)
- [23] J. AL-Zanganawee, S. Iftimie, T. Mubarak, A. Radu, O. Brincoveanu, S. Antohe, M. Enachescu, *Journal of Ovonic Research* **2**, 95 (2016)
- [24] A. Radu, S. Iftimie, V. Ghenescu, C. Besleaga, V.A. Antohe, G. Bratina, L. Ion, S. Craciun, M. Girtan, S. Antohe, *Digest Journal of Nanomaterials and Biostructures* **3**, 1141 (2011)
- [25] S. Iftimie, A. Radu, M. Radu, C. Besleaga, I. Pana, S. Craciun, M. Girtan, L. Ion, S. Antohe, *Digest Journal of Nanomaterials and Biostructures* **4**, 1631 (2011)
- [26] M.S. Dresselhaus, P.C. Eklund, *Advances in Physics* **49**, 705 (2000)
- [27] P.C. Eklund, J.M. Holden, R.A. Jishi, *Carbon* **33**, 959 (1995)
- [28] K.A. Wepasnick, B.A. Smith, J.L. Bitter, D.H. Fairbrother, *Analytical and Bioanalytical Chemistry* **3**, 1003 (2010)
- [29] R. Graupner, *Journal of Raman Spectroscopy* **38**, 673 (2007)
- [30] S. Hussain, P. Jha, A. Chouksey, R. Raman, S.S. Islam, T. Islam, P.K. Choudhary, *Journal of Modern Physics* **2**, 538 (2011)
- [31] E. Titus, N. Ali, G. Cabral, J. Gracio, P.R. Babu, M.J. Jackson, *Journal of Materials Engineering and Performance* **15**, 182 (2006)
- [32] J.-H. Du, J. Bai, H.-M. Cheng, *Polymer Letters* **5**, 253 (2007)
- [33] A.S. Ayesh, *Chinese Journal of Polymer Science* **4**, 537 (2010)